J. Fluid Mech. (1996), vol. 321, pp. 279–298

A mechanism for rivulet formation in heated falling films

By S. W. JOO[1], S. H. DAVIS[2] AND S. G. BANKOFF[3]

[1]School of Mechanical Engineering, Yeungnam University, Kyongsan, Korea

[2]Department of Engineering Sciences and Applied Mathematics, Northwestern University, Evanston, IL 60208, USA

[3]Department of Chemical Engineering, Northwestern University, Evanston, IL 60208, USA

(Received 22 July 1994 and in revised form 12 April 1996)

We consider a long-wave evolution equation that governs a draining film on a heated plate and hence is capable of describing both surface-wave and thermocapillary instabilities. When the flow and heat transfer rates are moderate, we show, via weakly nonlinear analysis of a truncated system and numerical simulation of the full nonlinear evolution equation, that coupled temporal instabilities can create surface deformations that lead to an array of rivulets aligned with the flow. This work thus demonstrates a mechanism of rivulet formation based solely on instability phenomena.

1. Introduction

A viscous liquid layer on a horizontal heated plane is susceptible to thermocapillary instabilities, caused by surface-tension variations at the liquid/gas interface. As summarized by Goussis & Kelly (1990), there are two different types of thermocapillary instabilities. One type, examined first by Pearson (1958), exists when thermal convection is significant, and occurs for disturbances wavelengths comparable to the layer thickness. This type does not require deformation of the interface. The other type, identified by Scriven & Sterling (1964), is always accompanied by surface deformations. Mean surface tension cuts off the short waves. For sufficiently thin layers, the effects of thermal convection are small, so that there is present only the long-wave instability associated with the free-surface deformation. Goussis & Kelly (1990) studied these two different types of instability in the presence of stabilizing hydrostatic pressures, and identified parametric regions where these can exist.

When the plane is tilted, the liquid drains downward due to gravity. If the layer thickness and the inclination angle are large enough to overcome the hydrostatic stabilization, another mode of instability is present, which occurs for isothermal layers and gives rise to formation of surface waves propagating downstream. This surface-wave instability, identified by Yih (1955, 1963) and Benjamin (1957), has been studied intensively for many years, as summarized by Lin (1983) and Lin & Wang (1985). Again, for sufficiently thin layers, the instability occurs for long waves, because short waves are suppressed by capillary forces.

Film flows coupling the aforementioned instabilities (falling film on a heated incline) have been studied often since the work of Lin (1975). Kelly, Davis & Goussis (1986) performed a linear stability analysis, and found a 'stability window' below and above which the flow becomes unstable due to thermocapillarity and mean flow, respectively.

This window exists due to the stabilizing effects of hydrostatic pressure. Goussis & Kelly (1991) extended the analysis, and identified the surface-wave and the two types of thermocapillary instabilities. They reckoned that the surface-wave and the long-wave thermocapillary instabilities reinforce each other, and the disturbance subject to these two instabilities takes the form of transverse waves, whereas that subject to thermocapillary instability of Pearson type assumes the form of longitudinal rolls. Burelbach, Bankoff & Davis (1988) considered sufficiently thin horizontal layers, and studied the long-wave instabilities by deriving an evolution equation of the Benney (1966) type for a two-dimensional layer. The effects of evaporative mass loss, vapour recoil, and van der Waals forces are incorporated. Joo, Davis & Bankoff (1991) generalized the study to include the effects of the mean flow in the absence of the van der Waals forces. They studied the nonlinear development of the flow by numerically integrating the long-wave evolution equation. They followed unstable evolutions to near rupture when the thermocapillary instability is dominant and towards wavebreaking when the surface-wave instability is dominant. For evolutions where the thermocapillary instability is significant, substantial local thinning of the layer is present and a characteristic double fingering occurs before rupture, leading to potential dryout at two points rather than one.

For a falling film on a heated surface, it is a common experience that dry spots are formed and are extended downstream, making the fluid flow around them. This breakdown of a thin liquid film into longitudinal streams has been a subject of investigation for many years. Hartley & Murgatroyd (1964) studied isothermal film flows, and discussed conditions under which the dry patch, once formed, will persist or be re-wetted. They considered two different models, dry-patch and rivulet models, which are, respectively, based on a force balance at the upstream stagnation point of a dry patch and a minimum total energy balance in a transversely unrestrained stream. Zuber & Staub (1966) extended the analysis to heated films, and incorporated thermocapillarity. Chung & Bankoff (1980) summarized these studies, and further generalized the theory to two-component flows to include the effects of non-zero surface shear stress.

In most of these studies on liquid-film breakdown, the mechanism initiating a dry patch is not discussed, and it is still an open question whether the thin-film instabilities discussed above are responsible for its initial development. For isothermal film flows, only the surface-wave instability is present, and this alone will not cause breakdown, since neither substantial local depression of a film (Joo *et al.* 1991) nor longitudinal patterns can develop. Therefore, if the thin film is to rupture and develop rivulets, then another mechanism must be present.

In the present study, we extend the two-dimensional study of Joo *et al.* (1991) and examine nonlinear evolutions of three-dimensional heated layers. We consider flows with small thicknesses and moderate heating, and thus focus on instabilities whose critical wavelength is much larger than the thickness of the layer. In particular, we show that the surface-wave and the long-wave thermocapillary instabilities interact nonlinearly with each other and can lead to surface corrugations in the form of longitudinal rolls, which would become rivulets after rupture. This constitutes a mechanism for the formation of longitudinal dry patches or rivulets.

We begin in §2 by introducing the evolution equation for a three-dimensional heated layer. In §3, we consider heated layers on a horizontal plane, and show the nonlinear evolution of three-dimensional heated layers in the absence of the mean flow. In §4, we incorporate the effect of mean flow by making the plane vertical. The effects of coupled instabilities are shown, including the formation of longitudinal rolls. We summarize the results in §5.

2. Long-wave theory

A Newtonian liquid of constant density ρ and viscosity μ is draining down a heated incline due to gravity. The layer is bounded above by the interface with a passive gas of ambient temperature T_∞. The bottom plane, inclined at an angle β with the horizontal, is kept at a constant temperature T_H.

The flow rate is controlled by changing the mean layer thickness d_0 and the angle β. The maximum velocity occurs at the interface, and for an undisturbed layer it is $gd_0^2 \sin\beta/(2\nu)$, where g is the gravitational acceleration and $\nu = \mu/\rho$. The Reynolds number R based on twice the surface velocity thus becomes $G \sin\beta$, where the parameter

$$G = \frac{d_0^3 g}{\nu^2} \tag{2.1}$$

is a measure of the layer thickness.

The temperature T_F at the interface is determined by convective heat losses to the ambient gas, and thus varies with the interfacial motion. The surface tension depends on temperature, and induces surface shear stresses; thermocapillarity is present. We assume that the surface tension σ decreases linearly with the temperature:

$$\sigma = \sigma_\infty - \gamma (T_F - T_\infty), \tag{2.2}$$

where σ_∞ is the surface tension at the ambient temperature T_∞. The constant γ $(= -\mathrm{d}\sigma/\mathrm{d}T)$ is positive for most common fluids, and measures the sensitivity of surface tension to temperature variations.

The reference surface tension σ_∞ can be parameterized as

$$\tilde{S} = \frac{\sigma_\infty d_0}{3\rho\nu^2}. \tag{2.3}$$

The intensity of heating ΔT $(\equiv T_H - T_\infty)$ affects the flow only through thermocapillarity (no buoyancy effects), and is measured by the Marangoni number,

$$M = \frac{\gamma d_0 \Delta T}{2\mu\kappa}, \tag{2.4}$$

where κ is the thermal diffusivity of the liquid layer. The heat transfer coefficient h_c between the liquid layer and the ambient gas is non-dimensionalized as the Biot number,

$$Bi = \frac{d_0 h_c}{k}. \tag{2.5}$$

The instabilities present, associated with the deformation of the interface, are long waves.† The characteristic length l in the streamwise or spanwise direction is much larger than the film thickness $(\epsilon \equiv d_0/l \ll 1)$. Therefore, the flow development can be described by the long-wave asymptotics of Benney type, which reduce the full system of the Navier–Stokes and the energy equations with appropriate boundary conditions to a single evolution equation. For a detailed derivation of the evolution equation for a two-dimensional layer, readers may refer to the work of Joo *et al.* (1991).

† As reported by Goussis & Kelly (1990), the thermocapillary instability of Pearson type requires sufficiently large intensity of heating, $M/Bi > 16.037$, and film thickness, $G \gg 1$. We consider flows with moderate heating $(M/Bi < 16.037)$ and small thickness $(G = O(1))$, so that the Pearson-type instability does not exist.

In a non-dimensional Cartesian coordinate system, the evolution equation for a three-dimensional layer is

$$h_t + Gh^2 h_x \sin\beta + \epsilon\left[\tfrac{2}{15}G^2\left(h^6 h_x\right)_x \sin^2\beta + \nabla\cdot\left\{\frac{BiM}{P}\left(\frac{h}{1+Bih}\right)^2 - \tfrac{1}{3}Gh^3\cos\beta\right\}\nabla h + S\nabla\cdot\left(h^3\nabla\nabla^2 h\right)\right] + O(\epsilon^2) = 0, \quad (2.6)$$

where $h(x, y, t)$ is the local layer thickness scaled by d_0, x and y are, respectively, streamwise and spanwise coordinates in units of d_0/ϵ, and time t is scaled by $\rho d_0^2/(\epsilon\mu)$. Here, $\nabla \equiv (\partial_x, \partial_y)$, the Prandtl number

$$P = \frac{\nu}{\kappa}, \quad (2.7)$$

and the surface-tension parameter $\tilde{S}$ is usually very large, and is rescaled to $S = \epsilon^2\tilde{S}$.

The second term in (2.6) describes the nonlinear-wave propagation. The third and fourth terms are responsible for the surface-wave and the thermocapillary instabilities, respectively. The fifth and sixth terms describe the stabilizing hydrostatic and capillary effects. The equation is highly nonlinear, and shows that the flow development is very sensitive to the local layer thickness.

The evolution equation (2.6) for an isothermal layer ($M = 0$) includes that obtained by Benney (1966), Krantz & Goren (1971), and Atherton & Homsy (1976) for two-dimensional layers ($\partial/\partial y = 0$) and Roskes (1970) and Krishna & Lin (1977) for three-dimensional layers. If we further set $\beta = 0$ (no mean flow) and make G negative, it describes Rayleigh–Taylor instability in thin viscous films with small Bond number (Yiantsios & Higgins 1989). If $\beta = 0$ and $Bi \to 0$, it describes the pure thermocapillary instability discussed by Davis (1983).

The linear stability analysis for a uniform basic state $h = 1$ is performed by considering an infinitesimal harmonic disturbance to the uniform layer:

$$h = 1 + Ae^{i(\boldsymbol{k}\cdot\boldsymbol{x} - \Gamma t)}, \quad (2.8)$$

where $0 \leqslant A \ll 1$, the wavenumber vector $\boldsymbol{k} = k(\cos\theta, \sin\theta)$, and complex frequency $\Gamma = \Gamma_R + i\Gamma_I$. Here, θ is an oblique angle, which is zero for two-dimensional (transverse) waves and $\pi/2$ for purely longitudinal modes. By substituting (2.8) into (2.6) and linearizing in A, one obtains the linearized phase speed

$$\Gamma_R = G\sin\beta \quad (2.9)$$

and the linear growth rate

$$\Gamma_I = \epsilon k^2\left[\tfrac{2}{15}G^2\cos^2\theta\sin^2\beta + \frac{BiM}{P(1+Bi)^2} - \tfrac{1}{3}G\cos\beta - Sk^2\right]. \quad (2.10)$$

The linear theory shows that the thermocapillarity ($M \neq 0$) does not affect the phase speed and that the two-dimensional waves are the preferred mode as in the isothermal layers. In §4, however, it will be shown that nonlinear modal interactions can lead to strikingly different conclusions.

Equation (2.10) clearly shows the destabilizing effects of mean flow and thermocapillarity and the stabilizing effects of hydrostatic pressure and mean surface tension. The surface-tension term has an extra factor k^2, and so provides the cutoff wavenumber k_c; disturbances with $k > k_c$ are suppressed by capillary forces. Figure 1 shows a linear stability diagram in an (M, G)-plane. The stable region exists due to hydrostatic effects. Therefore, as noted by Kelly *et al.* (1986), a stability window exists

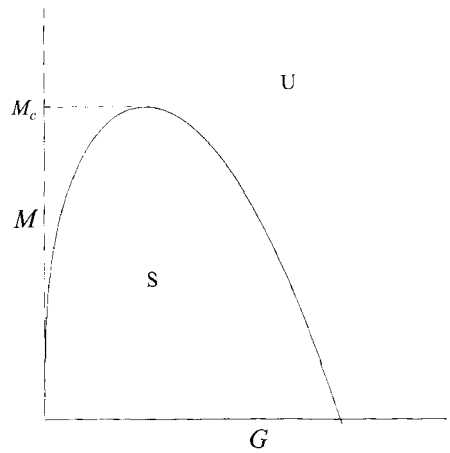

FIGURE 1. Linear stability diagram for heated inclined films, as given by Kelly *et al.* (1986). S: stable; U: unstable.

for non-vertical layers ($\beta \neq \pi/2$), which can be realized by keeping the intensity of heating M at a value smaller than M_c and varying the layer thickness G. The window disappears for sufficiently intense heating, $M > M_c$.

The nature of the instability can be analysed by introducing the absolute/convective instability concepts, summarized by Huerre & Monkewitz (1990). In convectively unstable flows, the growing disturbance wave moves away from its source, whereas in absolutely unstable flows, the instability contaminates the entire flow field. In isothermal film flows with small to moderate Reynolds numbers and physically realizable surface tensions $S > S_c$, the instability is convective. Here S_c is a critical value which usually is much smaller than the typical S for film flows. In the linear theory one can use the Gaster (1962) transformation to relate spatial and temporal growth. For a given forcing frequency one can examine temporal instability and access each wavenumber separately by examining the equivalent spatial growth of a disturbance. A detailed description of concepts and derivations is given by Huerre & Monkewitz (1990) or, for film flows, by Joo & Davis (1992). Liu, Paul & Gollub (1993) have shown experimently that isothermal film flows are convectively unstable. When a film flow is non-isothermal, there is no experimental or theoretical information on the absolute/convective nature of the flow. In the present work we examine the temporal response and find the appearance of longitudinal structures which would seem to be properly described by a temporal theory.

3. Thermocapillary instability

We now integrate (2.6) numerically and study the nonlinear evolution of unstable layers. We first consider flows on a horizontal heated layer ($\beta = 0$), and show the effects of the thermocapillary instability in the presence of hydrostatic and capillary forces. The effects of mean flow ($\beta \neq 0$) and the resulting coupled instabilities will be discussed in the following section.

The numerical scheme is a straightforward extension to three-dimensional layers of that used by Joo *et al.* (1991). The Hamming modified predictor-corrector method is used for temporal integration, with a Fourier spectral method for the spatial

derivatives. The computational domain $0 \leqslant x \leqslant 2\pi/k_1$ and $0 \leqslant x \leqslant 2\pi/k_2$ is one period of the initial disturbance

$$h(x, y, 0) = 1 - \delta_1 \cos(k_1 x) - \delta_2 \cos(k_2 y), \tag{3.1}$$

where $\delta_1 = \delta_2 = 0.1$, and k_1 and k_2 are, respectively, the streamwise and the spanwise wavenumbers. In all of the cases below, the parameter values are taken for illustration purposes only, and do not refer to any particular fluid system. In all of the figures shown, the x, y coordinates are scaled to make the large-aspect-ratio flow of comparable order in all directions.

Figure 2 shows the evolution of a horizontal layer when $G = 1$, $S = 1$, $Bi = 1$, $BiM/P = 5$, and $k_1 = k_2 = 0.5$. The wavenumbers, which correspond to approximately half of those for the maxinum linear growth rate in each direction, are appropriately chosen to show interesting secondary flow developments. The layer is unstable due to thermocapillarity. Figure 2(a) illustrates one period (both in x and y) of the initial disturbance (3.1). At the centre is the trough, which become shallower as the instability develops. The crests at four corners will increase in thickness. For a horizontal layer, there is no preferred direction. The thinning of the trough is accompanied by displacement in all directions of the fluid beneath the trough, which, in turn, induces higher lubrication pressure beneath the trough (see Joo *et al.* 1991). When the interface gets close to the bottom plate, this large pressure flattens the trough. Figure 2(b) shows one such state at $t = 60$. The trough has thinned to approximately 50% of the mean thickness, and the crest has grown to almost 145%. The trough stops thinning, and becomes blunt, and when the region near the edge of the flattened trough thins due to the thermocapillarity, a three-dimensional crater appears, surrounded by an axisymmetric finger. The centre of the flattened trough (the initial trough) continues to experience high pressure and eventually the interface bulges upward. Figure 2(c) shows the free-surface configuration at $t = 100$. The crests have continuously grown to 182% of the mean thickness, whereas the trough has grown upward to become a concave dome-shaped structure. The annular region near the edge of the dome has thinned to about 25% of the mean thickness. The pattern of the free surface for this state is well illustrated in Figure 2(d), which shows the contours of constant thickness.

After the layer ruptures, it is expected that the bulge at the centre would be isolated from the bulk film and would undergo secondary developments. The present calculation cannot describe the flow at or beyond rupture. Near rupture, the inertial and convective effects, as well as the long-range molecular forces, can be important (Burelbach *et al.* 1988), and so the evolution equation (2.6) ceases to model the flow adequately.

In figure 2, an axisymmetric evolution occurred because the wavenumbers k_1 and k_2 were equal. As discussed by Joo *et al.* (1991), the flow development, including the local thinning rate and the local thickness for the fingering, is very sensitive to the initial conditions. In three-dimensional layers, the two waves, characterized initially by k_1 and k_2, interact nonlinearly as they grow, so that different patterns result depending on the combination of the wavenumbers. Obviously, if one of the wavenumbers, say k_2, is too large, then the wave in the y- or spanwise direction disappears and a purely two-dimensional flow will development.

Figure 3 shows the evolution of the same layer as in figure 2, except that now $k_2 = 2k_1 = 1$. It shows the free-surface configuration at $t = 92.5$. On the crests, the local layer thickness is approximately 161% of the mean thickness, and the region around the bulge at the centre is near rupture. According to linear theory (2.10),

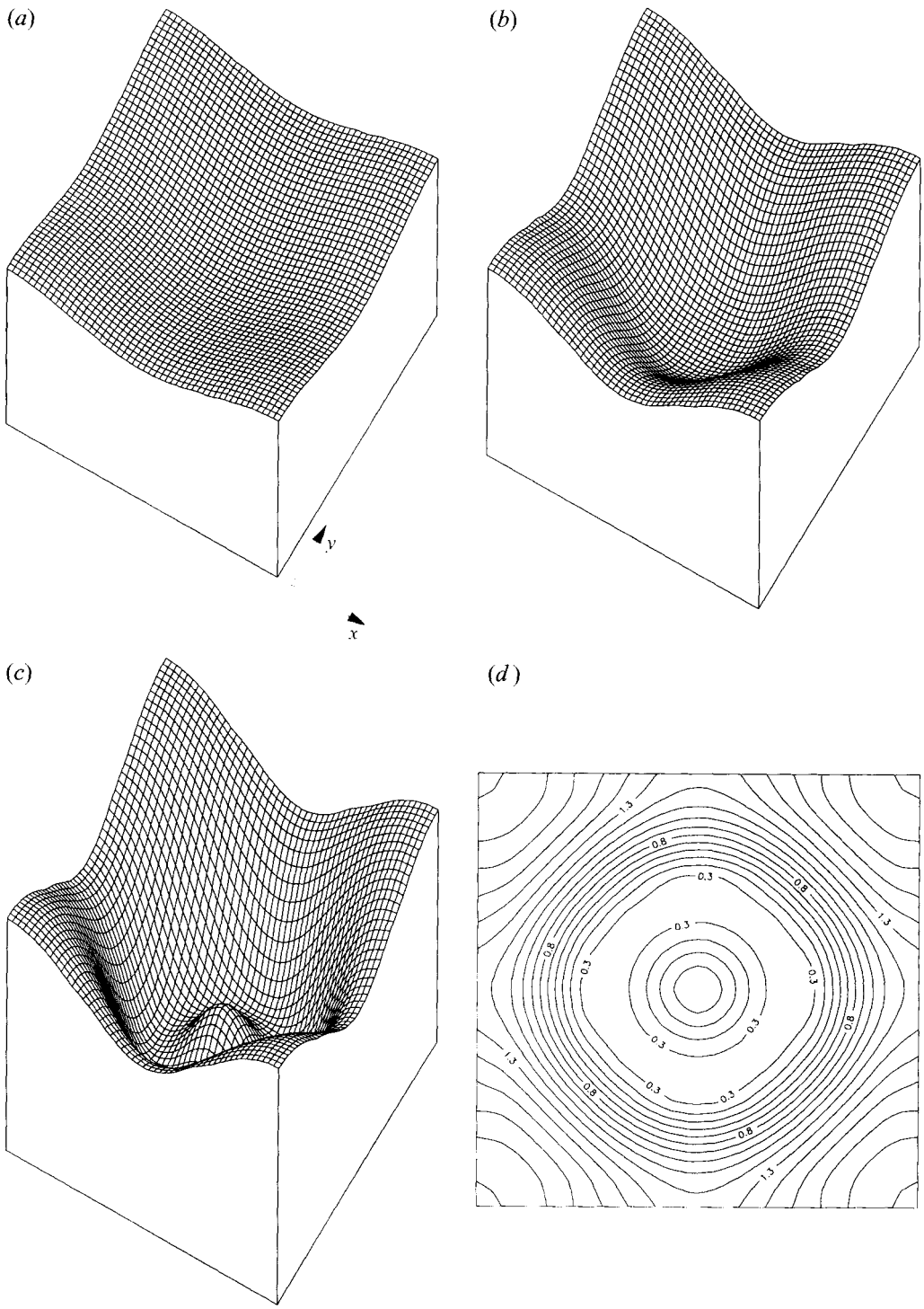

FIGURE 2. Nonlinear evolution of a heated horizontal layer when $G = 1$, $S = 1$, $Bi = 1$, $BiM/P = 5$ and $k_1 = k_2 = 0.5$. Free-surface configuration at (*a*) $t = 0$; (*b*) $t = 60$; (*c*) $t = 100$. And (*d*) contours of constant thickness at $t = 100$.

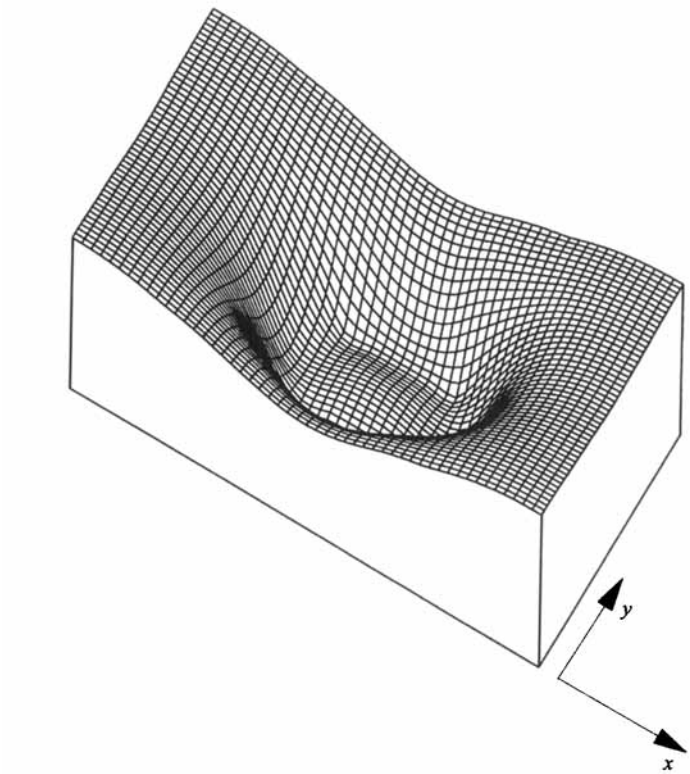

FIGURE 3. Nonlinear evolution of a heated horizontal layer when $G = 1$, $S = 1$, $Bi = 1$, $BiM/P = 5$, $k_1 = 0.5$ and $k_2 = 1$. Free-surface configuration at $t = 92.5$.

the wavenumber $k_2 = 1$ provides faster growth than $k_2 = 0.5$ of figure 2, and so the rupture time is now smaller in the nonlinear evolution. Near the tip of the bulge at the centre, the contours are ellipses elongated in the x-direction, compared to the circles in figure 2.

Thin films on a heated horizontal plate can become unstable due to the thermocapillarity. When the instability of the Pearson type is absent, an increase in film thickness enhances the hydrostatic stabilization. Therefore, the film has to be thin enough for the instability to occur. When the instability can occur, sufficiently long waves grow and significant local thinning results (in contrast to the isothermal surface-wave instability). After sufficient thinning, the trough flattens due to the lubrication effects, and eventually bulges upward due to the induced lubrication pressure. The pattern development thus depends strongly on the initial conditions. As discussed by Joo *et al.* (1991) for a two-dimensional heated layer, there is no saturation to a steady state; the local thinning persists until the film ruptures.

4. Coupled instabilities

The effects of mean flow and the surface-wave instability can be incorporated by tilting the bottom plate to a desired angle ($\beta \neq 0$). The presence of the surface-wave instability depends on the film thickness (or G) and the inclination angle β. Here, we present, as an example, the results for a vertical layer ($\beta = \pi/2$), where the

surface-wave instability is always present. Other cases indicate that the qualitative behaviour does not change substantially as the angle is decreased.

4.1. *Truncated-nonlinear analysis*

We first study the truncated-nonlinear behaviour of unstable layers by analysing a dynamical system derived from the evolution equation (2.6). The local layer thickness h is approximated by a finite Fourier series

$$h(x, y, t) = \sum_{m=-M}^{M} \sum_{n=-N}^{N} A_{mn} e^{ik_1 mx + ik_2 ny}. \tag{4.1}$$

Here, $A_{00} = 1$ from conservation of mass, and $A_{(-m)n} = A_{mn}^c$, where c denotes a complex conjugate. In the spanwise direction symmetry is always kept, so that $A_{m(-n)} = A_{mn}$.

By substituting (4.1) into the evolution equation and manipulating further, we obtain the following dynamical system for $M = N = 2$:

$$\left.\begin{aligned}
\dot{A}_{10} &= a_1 A_{10} + a_2 \left(|A_{10}|^2 + 2A_{01}^2\right) A_{10} + a_3 A_{10}^c A_{20} + a_4 A_{01} A_{11}, \\
\dot{A}_{01} &= b_1 A_{01} + b_2 \left(2|A_{10}|^2 + A_{01}^2\right) A_{01} + b_3 A_{01} A_{02} + b_4 \left(A_{10}^c A_{11} + A_{10} A_{11}^c\right), \\
\dot{A}_{20} &= c_1 A_{20} + c_2 A_{10}^2, \\
\dot{A}_{02} &= d_1 A_{02} + d_2 A_{01}^2, \\
\dot{A}_{11} &= e_1 A_{11} + e_2 A_{10} A_{01},
\end{aligned}\right\} \tag{4.2}$$

where the coefficients are listed in the Appendix.

4.2. *Nonlinear saturation*

In contrast to the horizontal layer with pure thermocapillary instability, there can be a nonlinear saturation of an initial unstable wave into a two-dimensional permanent wave. This permanent wave propagates at a constant nonlinear phase speed

$$c = G(1 + \alpha), \tag{4.3}$$

where the nonlinear contribution α is determined below. In the above truncated system, the permanent wave is represented by

$$\bar{h}(x') = 1 + 2|A_1| \cos(k_1 x') + 2|A_2| \cos(2k_1 x' + \phi), \tag{4.4}$$

where $x' = x - ct$ and ϕ is a constant. The values for $|A_1|$, $|A_2|$, c, α, and ϕ are obtained from the system (4.2) with $|\dot{A}_1| = |\dot{A}_2| = A_{01} = A_{02} = A_{11} = 0$. For example, we obtain, for the amplitude of the first mode,

$$|A_1|^2 = \frac{2k_1^2 G^2 \alpha^2 - c_{1r} a_{1r}}{2k_1^2 G^2 (2 + \alpha) + a_{2r} c_{1r} - a_{3r} c_{2r}}, \tag{4.5}$$

where the subscripts r and i denote real and imaginary parts, respectively. A detailed procedure for obtaining the equilibrated states for an isothermal layer is given by Gjevik (1970). If we neglect the nonlinear part α of the phase speed, set $M = 0$, and take only purely two-dimensional modes, equation (4.5) reduces to that obtained by Gjevik (1970) for a two-dimensional isothermal layer (see Lin 1983).

The condition for the nonlinear saturation (supercritical bifurcation) is obtained by requiring $|A_1|^2 \geqslant 0$, which gives the upper half of the wavenumbers unstable (closer

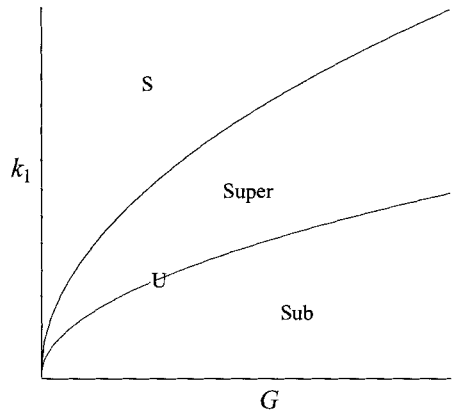

FIGURE 4. Nonlinear saturation of two-dimensional waves. Stability boundary (top curve) based on the linear theory of Yih (1963), and the bifurcation boundary (lower curve) based on the weakly nonlinear theory of Gjevik (1970).

to the cutoff value), as shown in figure 4. Longer disturbances do not satisfy this condition, and so the saturation does not occur (subcritical bifurcation) according to the truncated system (4.2).

Similar analysis can be performed in the search for permanent longitudinal rolls ($\partial_x = 0$). In (4.2), if we set $\dot{A}_{01} = \dot{A}_{02} = 0$ with the other modes set to zero, we obtain $b_1 d_1/(b_3 d_2 - b_2 d_1) \geqslant 0$ as the condition for saturation. This condition predicts a narrow band of spanwise wavenumber k_2 for some particular combinations of parameters. This band corresponds to wavenumbers much smaller than k_{2c}, in a region where the truncated system (4.2) is not a good approximation. Numerical verification with sixteen modes ($N = 6$) shows that the saturation to longitudinal rolls does not occur in this band (subcritical bifurcation). It thus appears that there is no saturation toward purely longitudinal rolls, which is also consistent with the fully nonlinear computation by Joo *et al.* (1991) for a two-dimensional pure thermocapillary instability and that in the previous section for a three-dimensional film.

4.3. *Three-dimensional instability*

Joo & Davis (1992) have shown that the two-dimensional permanent waves in isothermal layers are unstable to sufficiently long spanwise disturbances. This three-dimensional instability is seen by superposing an infinitesimal mixed-mode disturbance on the two-dimensional permanent wave:

$$h = \bar{h}(x') + \delta \left[H(x') e^{ik_2 y + \sigma t} + \text{c.c} \right], \tag{4.6}$$

where σ is now the growth rate of the three-dimensional modes. When (4.6) is substituted into the evolution equation (2.6) and the resulting equation is linearized in δ, an eigenvalue problem with periodic coefficients results. The growth rate σ then is obtained by using Floquet analysis.

An analogous analysis can be performed via the truncated system (4.2). If we write H in a finite Fourier series

$$H = \sum_{n=-2}^{2} D_n e^{ik_1 n x'}, \tag{4.7}$$

we notice that

$$A_{01} = D_0 e^{\sigma t} \quad \text{and} \quad A_{11} = D_1 e^{-ik_1 ct} e^{\sigma t} \tag{4.8}$$

while the D_2 (or A_{21}) mode is decoupled. Three real equations are then obtained from the truncated system (4.2), and the growth rate σ is obtained by solving the characteristic equation

$$\sigma = b_1 + 2\,|A_1|^2 \left[b_2 + b_4 \frac{e_{2r}(\sigma - e_{1r}) + 2k_1^2 G^2 \alpha}{(\sigma - e_{1r})^2 + k_1^2 G^2 \alpha^2} \right]. \tag{4.9}$$

For isothermal layers, the coefficients b_i are negative, so that purely spanwise modes would decay. However, the nonlinear interaction with the mixed mode transfers energy into the spanwise modes, in which case the numerator of the last term in (4.9) becomes negative. For layers with thermocapillarity, the coefficients b_i are positive for sufficiently small k_2, so that the spanwise modes would grow even in the absence of the two-dimensional wave. The three-dimensional instability will reinforce this thermocapillary instability.

Figure 5 shows the growth rate of a two-dimensional permanent wave subject to three-dimensional disturbances when $G = 5$, $BiM/P = 5$, $Bi = 0.1$, and $T = SG^{-1/3} = 1$. As a reference, the linear growth rate of purely spanwise disturbances is also plotted. The two cases shown, $k_1 = 1.9$ and $k_1 = 2.08$, are sufficiently close to the cutoff value $k_{1c} = 2.0895$ for the truncated system to be an appropriate approximation. The case for $k_1 = 1.9$ clearly shows the additional effect of the three-dimensional instability over the spanwise thermocapillary instability. The growth rate is substantially increased, and the cutoff spanwise wavenumber for instability is also larger. The wavenumber $k_1 = 2.08$ is very close to the cutoff value. The two-dimensional permanent wave is virtually monochromatic and its amplitude is very small. The effect of the three-dimensional instability thus is less pronounced. Near $k_2 = 0$ the growth rate is higher than the corresponding purely spanwise mode due to the three-dimensional instability. The capillary stabilization of the three-dimensional mode occurs at a smaller spanwise wavenumber than that of the purely longitudinal mode, so that the cutoff value for the overall instability is decreased slightly due to the three-dimensional instability.

The nonlinear behaviour of a heated draining film predicted by a truncated system exhibits interesting differences from, as well as similarities to, that of an isothermal layer. As in an isothermal layer, there is a tendency toward a permanent two-dimensional wave. This two-dimensional wave is unstable to three-dimensional disturbances due to a three-dimensional instability, which also exists in isothermal layers, and the thermocapillary instability. Owing to the additional effects of the thermocapillarity, the three-dimensional modes would grow more rapidly than in an isothermal layer. There is no nonlinear saturation resulting from the balance between the destabilizing thermocapillarity and the stabilizing mean surface tension. The spanwise mode thus will continue to grow, while the streamwise modes tend to saturate. It is then expected that a longitudinal pattern would develop as the layer drains down further. Again, the longitudinal rolls will not saturate but presumably grow until the film ruptures and dry patches form. In order for the thermocapillarity to sustain the local thinning of the longitudinal rolls, the spanwise wavenumber has to be sufficiently small, as shown also in figure 5. This provides the ranges for the resultant size (width) of the rivulets. The spanwise wavenumber that corresponds to the maximum growth rate may give the approximate size of the rivulets. The exact scale of the rivulets or the dry patches for a particular choice of parameters,

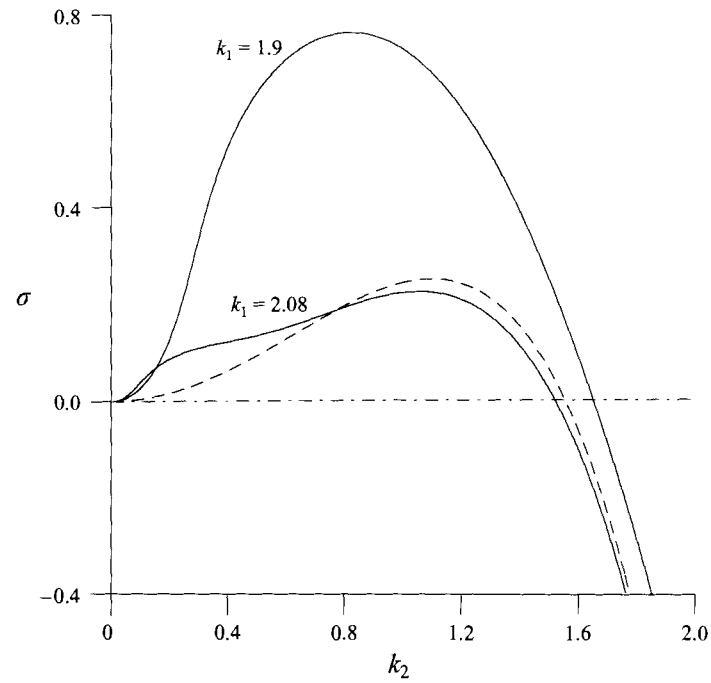

FIGURE 5. Three-dimensional instability of heated draining films when $G = 5$, $BiM/P = 5$, $Bi = 0.1$ and $T = SG^{-1/3} = 1$. The broken line shows the corresponding growth rate for purely spanwise disturbances.

however, should be determined by fully nonlinear analysis of the original coupled system. Contrary to those in horizontal layers, shown in the previous section, the rupture spots or the dry patches will be aligned with the flow direction, presumably resulting in an array of rivulets.

The truncated-nonlinear analysis thus shows that the thermocapillarity can trigger spontaneous formation of rivulets in thin draining films. Owing to the interaction with the mean flow, surface waves in a thin film tend to saturate to form nonlinear transverse waves, which are in turn unstable to three-dimensional disturbances. For isothermal films the growth of the three-dimensional modes is bounded, and periodic or quasi-periodic waves result; films stay continuous. In the presence of the thermocapillarity, however, there is an unbounded growth in the three-dimensional modes. Cross-stream the balancing forces are those due to the thermocapillarity, surface tension, and hydrostatic pressure (for a non-vertical film). As also shown by Krishnamoorthy, Ramaswamy & Joo (1995) via a series of full-scale numerical integration of the original fully coupled system, this combination does not lead to nonlinear saturation; all thin films subject to purely thermocapillary instability of the interfacial mode rupture. The wave amplitude in the spanwise direction thus continues to grow, while that in the streamwise direction tends to stay bounded. More and more energy is brought into the spanwise depression, and the film would eventually rupture to form longitudinal dry patches and rivulets. An extensive nonlinear numerical study is required to obtain the range of parameters over which the rivulet formation occurs, and will be a subject of subsequent reports. In what follows, we present a few generic cases that show the evolution toward rivulets by numerically integrating the full evolution equation.

4.4. *Spectral computation*

We study the nonlinear flow developments by integrating the evolution equation (2.6) using the Fourier-spectral method explained above.

In figure 6, the evolution of a vertical layer is shown when $G = 1$, $S = 1$, $Bi = 1$, $BiM/P = 5$. The parameters chosen are identical to those in figures 2 and 3 except that now $\beta = \pi/2$. The wavenumbers of the initial disturbance $k_1 = k_2 = 0.5$ are the same as in figure 2, so figure 2(*a*) again shows the initial profile of the free surface. As the liquid flows downstream, the disturbance grows in time due to the surface-wave and thermocapillary instabilities. In the initial stages, the surface-wave instability appears to dominate, and the flow development is similar to that of isothermal layers. Figure 6(*a*) shows the state at $t = 15$. The local phase speed is proportional to the square of the local film thickness according the evolution equation (2.6), so that the crests travel faster than the troughs. If the layer were isothermal and thus the thermocapillary instability were absent, the surface wave would evolve without substantial local thinning near the trough (Joo *et al.* 1991). In the presence of the thermocapillary instability, however, the local thinning persists until the layer ruptures. Figure 6(*b*) shows the free-surface configuration at $t = 30$. The thermocapillary instability is important, and begins to dictate the growth of the three-dimensional modes. The two-dimensional modes (transverse waves) are affected by the mean flow, which seems to neutralize the local thinning of the thermocapillary instability. This becomes more obvious as the flow develops further, as shown in figure 6(*c*) for $t = 60$. The growth of three-dimensional modes causes significant reduction of the local film thickness along the centreline parallel along the flow direction. The fluid is continuously displaced laterally from this centreline to the thicker region, further preventing the growth of the streamwise structure except near the centreline. Although three-dimensional development near the centreline is present, the overall pattern clearly shows the development of longitudinal structures. There is a trough of thickness of approximately 50% of the mean film thickness along the centreline, and along the edges are the crests. When the layer is allowed to evolve further, lubrication pressure creates the characteristic fingering, as shown in figure 6(*d*). The tips of the fingers (the two new troughs) have thinned to about 20% of the mean thickness. After these thin further and rupture, we expect to observe spatially periodic rivulets separated by dry regions which run parallel to the flow direction.

This rivulet formation has two very important implications. Firstly, it explains for the first time a possible mechanism for the creation of dry patches and rivulets from continuous films. Although there have been countless studies on rivulets, an understanding of the evolution toward rivulet formation has been lacking. The present mechanism depends on coupled instabilities, and thus does not apply to isothermal layers. Secondly, neither of the two instabilities by itself has tendency to develop longitudinal patterns. It is only when the two interact properly that the longitudinal structures result. If the surface wave is dominant, the nonlinear flow developments will be similar to those for isothermal layers, which exhibit aperiodic three-dimensional waves propagating downstream. On the other hand, if the thermocapillary instability dominates, the evolutions will not display a preferred direction. A thorough numerical search is required to identify the parameteric regions for the formation of longitudinal patterns. As in many other cases related to pattern selection, the linear theory is unable to predict these formations.

Many previous studies of rivulets focus on fully developed states, and have proposed models for their size and stability. The present approach does not yet allow

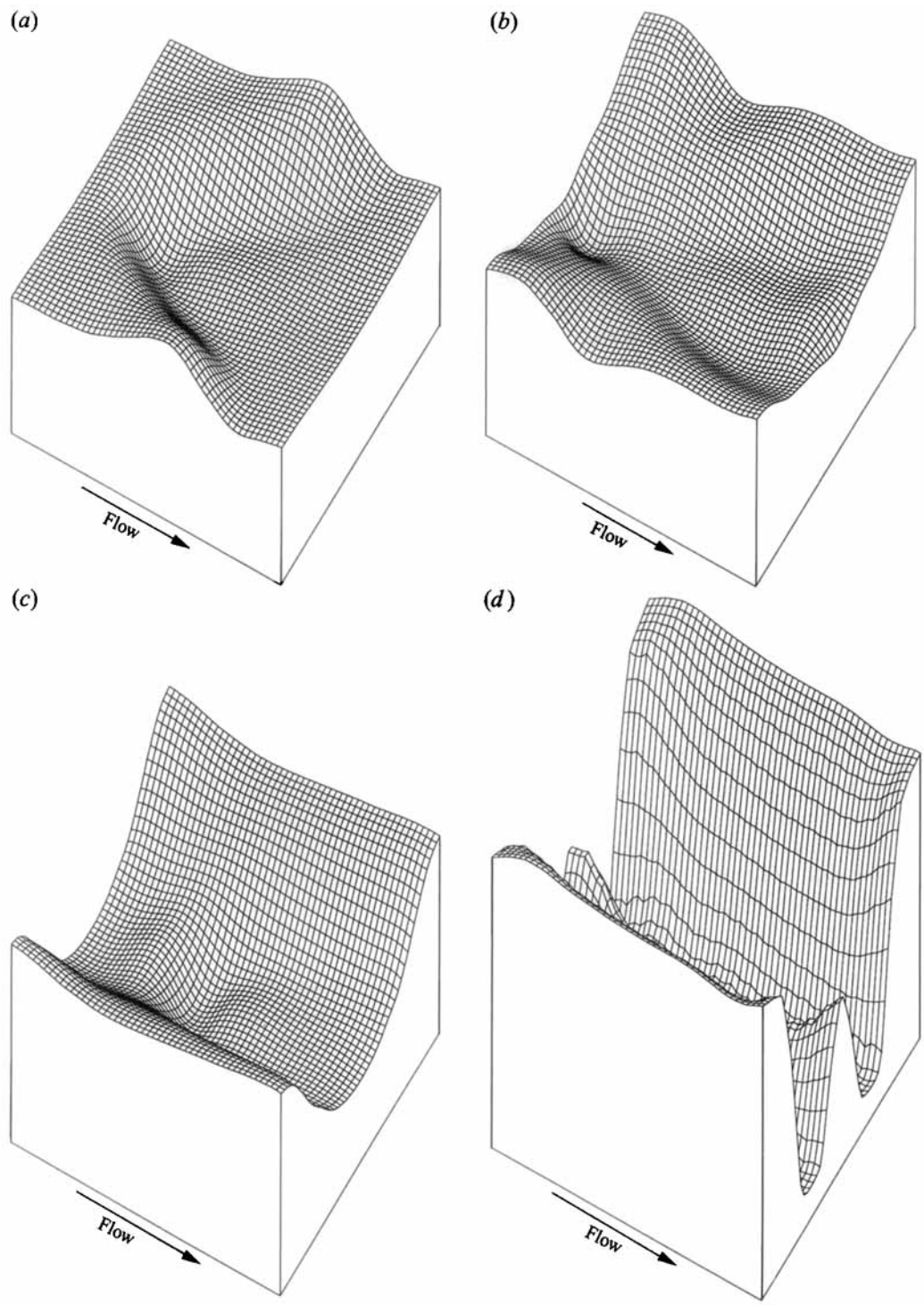

FIGURE 6. Nonlinear evolution of a heated vertical layer when $G = 1$, $S = 1$, $Bi = 1$, $BiM/P = 5$ and $k_1 = k_2 = 0.5$. Free-surface configuration at (*a*) $t = 15$; (*b*) $t = 30$; (*c*) $t = 60$; (*d*) $t = 97$.

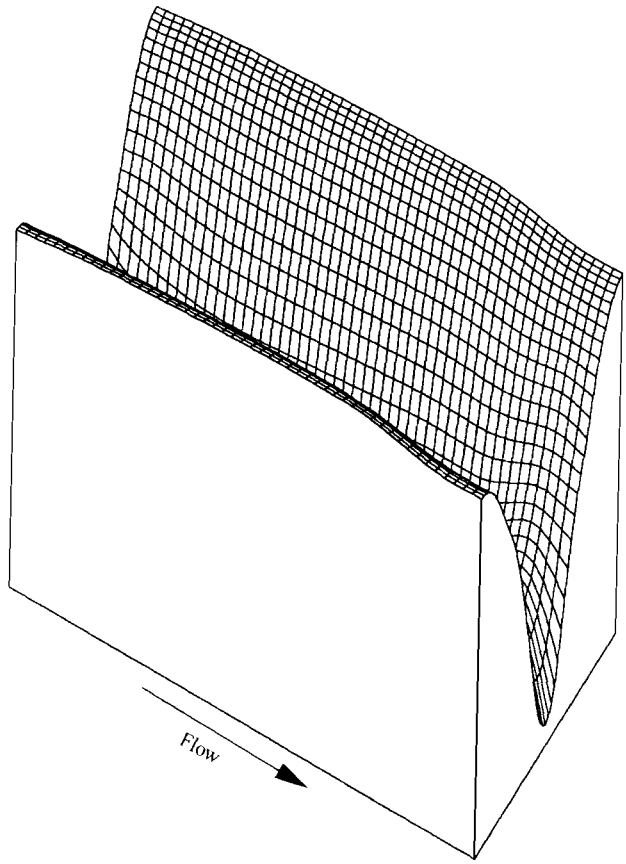

FIGURE 7. Nonlinear evolution of a heated vertical layer when $G = 1$, $S = 1$, $Bi = 1$, $BiM/P = 5$, $k_1 = 0.5$ and $k_2 = 1$. Free-surface configuration at $t = 60$.

us to analyse these final states, since the computation must be terminated before the layer ruptures.

Figure 7 shows another evolution toward rivulets with the spanwise wavenumber $k_2 = 1$; all other parameters are identical to those in figure 6. The growth of spanwise modes due to the thermocapillary instability is faster than that in the previous case. The formation of a longitudinal pattern is already seen at $t = 30$. The troughs and crests are, respectively, about 57% and 131% of the mean film thickness. Fingering does not occur until the layer almost ruptures, consistent with the two-dimensional evolutions reported by Joo *et al.* (1991). We show the free-surface configuration at $t = 60$. The thinnest region is approximately 9% of the mean thickness, and the fingering is about to occur. Compared to the previous case, local thinning is enhanced, resulting in a smaller rupture time. If fingering occurs, it would be at a later stage of the evolution, so that the bulge along the centre accompanying the fingering would be much smaller than that in the previous case of $k_2 = 0.5$. The configuration of rivulets thus is different than in the previous evolution.

In figure 8, the spanwise wavenumber is decreased to 0.25, with the other parameters unchanged. Local thinning rates are smaller than those in the previous cases of shorter spanwise wavelengths, and so the rupture time is increased. The fingering occurs at a much earlier stage of the evolution, so that the rolls along the centreline are much larger.

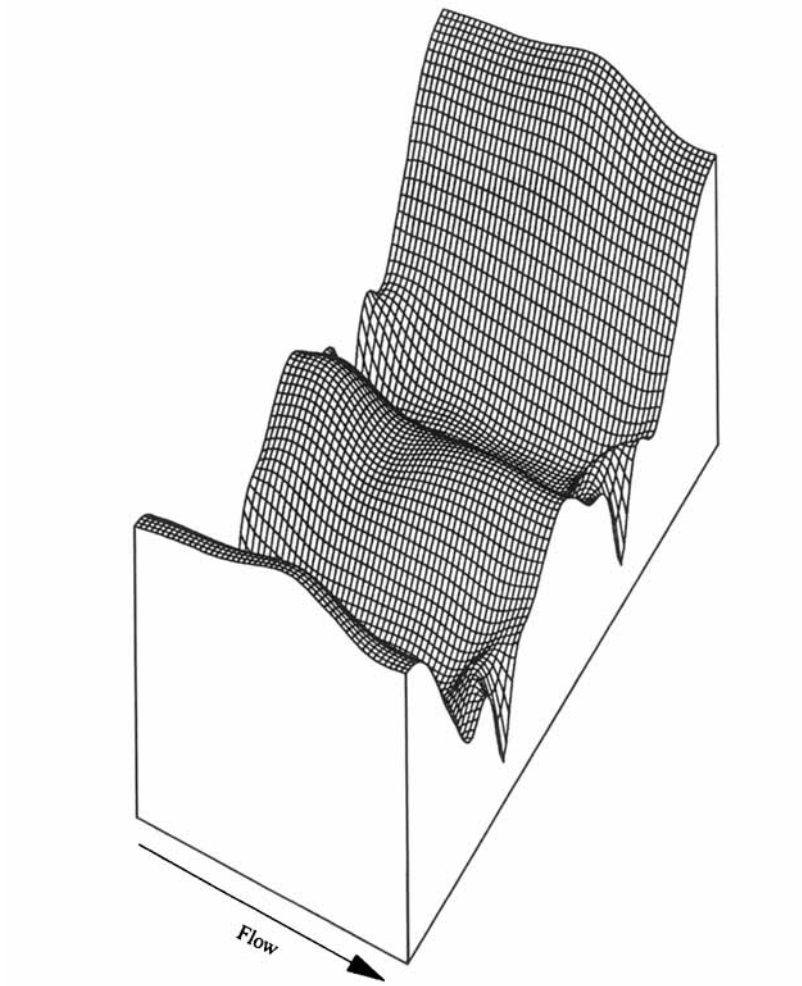

FIGURE 8. Nonlinear evolution of a heated vertical layer when $G = 1$, $S = 1$, $Bi = 1$, $BiM/P = 5$, $k_1 = 0.5$ and $k_2 = 0.25$. Free-surface configuration at $t = 175$.

Thus, when the heated layer is tilted, and the thermocapillary instability is coupled with the surface-wave instability, longitudinal rolls can evolve through nonlinear interactions of the two different modes. As the flow develops further and the layer ruptures, rivulets can be formed. The initial shape and size of these rivulets depend strongly on the disturbance wavenumbers, as well as other parameters.

5. Concluding remarks

The nonlinear behaviour of thin liquid layers is studied by numerically integrating a long-wave evolution equation of Benney type which includes the effects of viscosity, gravity, capillarity, thermocapillarity, and inertia.

The horizontal layers have no surface-wave instability, and evolve from the effects of small disturbances with no preferred direction parallel to the wall. If, say, two-dimensional disturbances are imposed, an initial interfacial depression will deepen, flatten due to lubrication pressures (Joo *et al.* 1991), and then evolve into a sym-

metric pair of fingers that approach the wall. If the imposed disturbances are, say, axisymmetric, the fingers that develop constitute an axisymmetric crater that further develops. In any case the rupture should not occur at a single point but an a 'ring' that isolates an island of fluid from the remainder of the film. The evolution depends on the initial disturbance and the size of the periodic box for numerical computation.

Inclined isothermal layers become two-dimensional, as determined by linear theory, but develop complicated three-dimensional wave systems when nonlinearity is considered. Two-dimensional permanent waves can exist, but are always unstable to three-dimensional perturbations for vertical layers (Joo & Davis 1992).

The inclined heated layers (coupled instabilities) evolve in marked contrast with the linear theory. For the first time it has been shown that the two instability modes can interact nonlinearly and give rise to longitudinal patterns alien to each of the two modes alone. In effect, the mean flow hinders the growth of the two-dimensional modes, and slows the local thinning. In the spanwise direction, the mean flow is absent, and the thinning due to the thermocapillary instability is effective. The growth of spanwise-periodic modes generates longitudinal rolls, which will evolve toward rivulets after the layer ruptures. Again, as the spanwise-periodic mode grows, the flattening and the fingering occur before rupture, owing to lubrication-pressure effects. Therefore, in one spanwise period, two rivulets can result, which are, for horizontal layers, analogous to an island surrounded by bulk fluid. The shape and size of the rivulets are again sensitive to the wavenumbers of the initial disturbance.

The longitudinal patterns mentioned above can develop only when the two instability modes have moderate intensity and are appropriately balanced. If the flow rate is too large compared to the intensity of heating, the surface-wave instability will dominate. If the heating is too strong, the thermocapillary instability dominates. When both instability modes are too strong and thus the flow is highly unstable, the local thinning due to the thermocapillary instability and the wave steepening due to the surface-wave instability reinforce each other, resulting in large local slope or incipient wave breaking. The evolution equation (2.6) then no longer describes the flow properly.

The present numerical experiments were performed in a spatially periodic domain. As initial perturbations, we have used localized bumps or alternatively three-dimensionally perturbed oblique waves, but have not encountered drastically different behaviours. As discussed by Joo & Davis (1991) for isothermal layers, the subharmonics of a fundamental disturbance mode are also linearly unstable, and sometimes can lead to chaos. If we allow subharmonic disturbances in the spanwise or streamwise modes, the evolution of the heated layers may be more complex than that reported here.

The instabilities in a thin draining film occur in the form of free-surface deformations. For isothermal films, the primary surface-wave instability can lead to nonlinear saturation, resulting in transverse permanent waves. A secondary three-dimensional instability tend to transform these waves into three-dimensional aperiodic waves. For films with thermocapillary, the transverse saturation exists, but the tendency toward three-dimensional patterns is much stronger. Since there is no spanwise saturation, the three-dimensional instability coupled with the thermocapillary instability would lead to an array of rivulets aligned with the flow.

The next step, given the mechanism presented, is to quantify the longitudinal structures for given liquids, tilt angles, and flow and heating rates with the object of predicting the scales of the rivulets to be expected. This will be the subject of a subsequent communication.

We have described a possible theory for the development of longitudinal structure for films having small flow rates and small heat fluxes. This theory is a dynamic one that shows how longitudinal structure develops from general initial conditions. This structure is found to be on a transverse scale comparable to the downstream scale. In the case of a channel flow heated from below where there is buoyancy-driven convection only, longitudinal structure develops and the flow is attracted to this stable equilibrium (see Kelly 1994). In the present case, longitudinal rolls are not an equilibrium solution since they develop under the influence of thermocapillary forces. Pure thermocapillary instability does not equilibrate but yet the flow is attracted to such structure.

There are no detailed experiments for low flow rates and low heat fluxes with which to compare our theory. However, there has been recent work on the direct simulation of heated falling films in which no long-wave approximation is utilized. Krishnamoorthy, Ramaswamy & Joo (1996) show that the results obtained in the present work are quantitatively correct for small enough G and M. Careful experiments on flow patterns or computations for detailed comparisons would be welcome.

This work was supported by the US Department of Energy, Division of Basic Energy Sciences, through Grant no. DE FG02-86ER13641.

Appendix. Coefficients of equations (4.2)

$$a_1 = -\mathrm{i}k_1 G + \epsilon k_1^2 \left[\frac{2}{15}G^2 + \frac{BiM}{P(1+Bi)^2} - k_1^2 S\right],$$

$$a_2 = -\mathrm{i}k_1 G + \epsilon k_1^2 \left[2G^2 + \frac{BiM(1-2Bi)}{P(1+Bi)^4} - 3k_1^2 S\right],$$

$$a_3 = -2\mathrm{i}k_1 G + \epsilon k_1^2 \left[\frac{4}{5}G^2 + \frac{2BiM}{P(1+Bi)^3} - 21k_1^2 S\right],$$

$$a_4 = -4\mathrm{i}k_1 G + 2\epsilon k_1^2 \left[\frac{4}{5}G^2 + \frac{2BiM}{P(1+Bi)^3} - 3(k_1^2+k_2^2)S\right],$$

$$b_1 = \epsilon k_2^2 \left[\frac{BiM}{P(1+Bi)^2} - k_2^2 S\right], \quad b_2 = \epsilon k_2^2 \left[\frac{BiM(1-2Bi)}{P(1+Bi)^4} - 3k_2^2 S\right],$$

$$b_3 = \epsilon k_2^2 \left[\frac{2BiM}{P(1+Bi)^3} - 21k_2^2 S\right], \quad b_4 = \epsilon k_2^2 \left[\frac{2BiM}{P(1+Bi)^3} - 3(k_1^2+k_2^2)S\right],$$

$$c_1 = -2\mathrm{i}k_1 G + 4\epsilon k_1^2 \left[\frac{2}{15}G^2 + \frac{BiM}{P(1+Bi)^2} - 4k_1^2 S\right],$$

$$c_2 = -2\mathrm{i}k_1 G + 2\epsilon k_1^2 \left[\frac{4}{5}G^2 + \frac{2BiM}{P(1+Bi)^3} - 3k_1^2 S\right],$$

$$d_1 = 4\epsilon k_2^2 \left[\frac{BiM}{P(1+Bi)^2} - 4k_2^2 S\right], \quad d_2 = 2\epsilon k_2^2 \left[\frac{2BiM}{P(1+Bi)^3} - 3k_2^2 S\right],$$

$$e_1 = -\mathrm{i}k_1 G + \epsilon \left[\frac{2}{15}k_1^2 G^2 + (k_1^2+k_2^2)\frac{BiM}{P(1+Bi)^2} - (k_1^2+k_2^2)^2 S\right],$$

$$e_2 = -2\mathrm{i}k_1 G + \epsilon \left[\frac{4}{5}k_1^2 G^2 + (k_1^2+k_2^2)\frac{2BiM}{P(1+Bi)^3} - 3(k_1^4+k_2^4)S\right].$$

REFERENCES

ATHERTON, R. W. & HOMSY, G. M. 1976 On the derivation of evolution equations for interfacial waves. *Chem. Engng Commun.* **2**, 57–77.

BENJAMIN, T. B. 1957 Wave formation in laminar flow down an inclined plane. *J. Fluid. Mech.* **2**, 554–574.

BENNEY, D. J. 1966 Long waves on liquid films. *J. Math. & Phys.* **45**, 150–155.

BURELBACH, J. P., BANKOFF, S. G. & DAVIS, S. H. 1988 Nonlinear stability of evaporating/condensing liquid films. *J. Fluid Mech.* **195**, 463–494.

CHUNG, J. C. & BANKOFF, S. G. 1980 Initial breakdown of a heated liquid film in cocurrent two-component annular flow: II. Rivulet and Drypatch models. *Chem. Engng Commun.* **4**, 455–470.

DAVIS, S. H. 1983 Rupture of thin liquid films. In *Waves on Fluid Interfaces* (ed. R. E. Meyer), pp. 291–302. Academic.

GASTER, M. 1962 A note on the relation between temporary-increasing and spatially-increasing disturbances in hydrodynamic stability. *J. Fluid Mech.* **14**, 222–224.

GJEVIK, B. 1970 Occurrence of finite-amplitude surface waves on falling liquid films. *Phys. Fluids* **13**, *1918–1925.*

GOUSSIS, D. A. & KELLY, R. E. 1990 On the thermocapillary instabilities in a liquid layer heated from below. *Intl J. Heat Mass Transfer* **33**, 2237–2245.

GOUSSIS, D. A. & KELLY, R. E. 1991 Surface wave and thermocapillary instabilities in a liquid film flow. *J. Fluid Mech.* **223**, 25–45.

HARTLEY, D. E. & MURGATROYD, W. 1964 Criteria for the breakup of thin liquid layers flowing isothermally over solid surfaces. *Intl J. Heat Mass Transfer* **7**, 1003–1015.

HUERRE, P. & MONKEWITZ, P. A. 1990 Local and global instabilities in spatially developing flows. *Ann. Rev. Fluid Mech.* **22**, 473–537.

JOO, S. W. & DAVIS, S. H. 1992 Instabilities of thee-dimensional viscous falling films. *J. Fluid Mech.* **242**, 529–547.

JOO, S. W. & DAVIS, S. H. 1992 Irregular waves on viscous falling films. *Chem. Engng Commun.* **118**, 111–123.

JOO, S. W., DAVIS, S. H. & BANKOFF, S. G. 1991 Long-wave instabilities of heated falling films: two dimensional theory of uniform layers. *J. Fluid Mech.* **230**, 117–146.

KELLY, R. E. 1994 The onset and development of thermal convection in fully developed shear flows. *Adv. Appl. Mech.* **31**, 35–112.

KELLY, R. E., DAVIS, S. H. & GOUSSIS, D. A. 1986 On the instability of heated film flow with variable surface tension. *Proc. 8th Intl Heat Transfer Conf.* **4**, 1937–1942.

KRANTZ, W. B. & GOREN, S. L. 1971 Stability of thin liquid films flowing down a plane. *Indust. Engng Chem. Fundam.* **10**, 91–101.

KRISHNA, M. V. G. & LIN, S. P. 1977 Nonlinear stability of a viscous film with respect to three-dimensional side-band disturbances. *Phys. Fluids* **20**, 1039–1044.

KRISHNAMOORTHY, S., RAMASWAMY, B., & JOO, S. W. 1995 Spontaneous rupture of thin liquid films due to thermocapillarity; A full-scale direct numerical simulation. *Phys. Fluids* **7**, 2221–2223.

KRISHNAMOORTHY, S., RAMASWAMY, B. & JOO, S. W. 1996 Nonlinear wave formation and rupture in heated falling films: a full-scale direct numerical simulation. *J. Fluid Mech.* (submitted).

LIN, S. P. 1975 Stability of liquid flow down a heated inclined plane. *Lett. Heat Mass Transfer* **2**, 361.

LIN, S.-P. 1983 Film waves. In *Waves on Fluid Interfaces* (ed. R. E. Meyer), pp. 262–289. Academic.

LIN, S.-P. & WANG, C.-Y. 1985 Modelling wavy film flows. In *Encyclopedia of Fluid Mechanics*, vol. 1, pp. 931–951. Gulf.

LIU, J., PAUL, J. D. & GOLLUB, J. P. 1993 Measurements of the primary instabilities of film flows. *J. Fluid Mech.* **250**, 69–101.

PEARSON, J. R. A. 1958 On convection cells induced by surface tension. *J. Fluid Mech.* **4**, 489–500.

RUSKES, G. J. 1970 Three-dimensional long waves on a liquid film. *Phys. Fluids* **13**, 1440–1445.

SCRIVEN, L. E. & STERLING, C. V. 1964 On cellular convection driven surface tension gradients: effects of mean surface tension and surface viscosity. *J. Fluid Mech.* **19**, 321–340.

YIANTSIOS, S. G. & HIGGINS B. G. 1989 Rayleigh-Taylor instability in thin viscous films. *Phys. Fluids* A **1**, 1484–1501.

YIH, C.-S. 1955 Stability of parallel laminar flow with a free surface. *Proc. 2nd US Congr. Appl. Mech.*, pp. 623–628. ASME.

YIH, C.-S 1963 Stability of liquid flow down an inclined plane. *Phys. Fluids* **6**, 321–334.

ZUBER, N. & STAUB, F. W. 1966 Stability of dry patches forming in liquid films flowing over heated surfaces. *Intl J. Heat Mass Transfer* **9**, 897.